

SUPPORTING INFORMATION

Perturbation of clopyralid on bio-denitrification and nitrite accumulation: Long-term performance and biological mechanism

Suyun Sun^{a,b}, Ya-Nan Hou^{a,b*}, Wei Wei^c, Hafiz Muhammad Adeel Sharif^d, Cong Huang^b, Bing-Jie Ni^c, Haibo Li^a, Yuanyuan Song^a, Caicai Lu^a, Yi Han^a, Jianbo Guo^{a*}

a Tianjin Key Laboratory of Aquatic Science and Technology, School of Environmental and Municipal Engineering, Tianjin Chengjian University, Tianjin 300384, China

b National Technology Innovation Center of Synthetic Biology, Tianjin Institute of Industrial Biotechnology, Chinese Academy of Sciences, Tianjin 300308, China

c Centre for Technology in Water and Wastewater, School of Civil and Environmental Engineering, University of Technology Sydney, Sydney, NSW 2007, Australia

d College of Chemistry and Environmental Engineering, Shenzhen University, Shenzhen 518060, China

Summary

Pages: 7 ; Figures: 4; Tables: 2

.

Methods

1. Composition of trace element solution

Trace element solution was prepared dissolving (g/L): 1.50 FeCl₃·6H₂O, 0.12 MnCl₂·4H₂O, 0.03 CuSO₄·5H₂O, 0.15 H₃BO₃, 0.18 KI, 0.06 Na₂MoO₄·2H₂O, 0.15 CoCl₂·6H₂O, 0.12 ZnSO₄·7H₂O, 10 EDTA [1].

2. CLP determination

CLP was measured by high-performance liquid chromatography (HPLC, LC-1260, Agilent, USA) with ZORBAX SB-C18 column (250 mm × 4.6 mm × 5 μm) and UV-Vis detector. The detector wavelength was set at 225 nm and 30 μL sample was injected. The mobile phase was a mixture of acetonitrile and water (3:7, v/v) at a flow rate of 1.0 mL/min, and the water was acidified with 0.1% H₃PO₄.

3. ETSA assay

Election transport system activity (ETSA) was measured according to the described protocol [2]. A mixture of 2 mL samples (washed three times with PBS solution) and 1 mL 0.2 % 2-(4-Iodophenyl)-3-(4-nitrophenyl)-5-phenyltetrazolium chloride (INT) solution was added, and then incubated in a rotary incubator (150 rpm) at 35 °C for 30 min in darkness. The reaction mixture was added 1 mL 37 % methanol to stop enzyme reaction, then the reaction mixture was centrifuged (4000 rpm, 5 min, 25 °C) to discard the supernatant. 5 mL methanol was added to extract the produced triphenyl formazan, and incubated in a rotary incubator at 35 °C for 5 min with continual agitation at 150 rpm/min in darkness. After centrifugation at 4000 rpm for 5 min to collect the supernatants, absorbance of the formed INT-formazan was immediately recorded by ultraviolet spectrophotometer (UV-2700, Shimadzu, Japan) at 485 nm against a methanol solvent blank. The electrons produced by the microbe can react with electron acceptor INT to produce triphenyl formazan. The ETSA value was calculated as follows:

$$INT - ETSA = \frac{D_{485}V}{k_i W t}$$

where D_{485} is the absorbance value of sample; V (mL) is extractant volume; k_i (0.0547) is the slope of the standard curve for triphenyl formazan; W (mg) is microbial dry

weight and t (h) is culture time after adding INT.

4. ATP assay

Adenosine triphosphate (ATP) was measured according to the described protocol [3]. After washed three times with PBS solution and collected by centrifugation (4000 rpm, 10 min, 25 °C), 1 mL samples were resuspended in 6 mL Tris-EDTA buffer solution, and then boiled for 3 min. After cooled to room temperature (25 °C), the solution was centrifuged at 8000 rpm for 5 min and filtered through 0.22 μm filter membranes for analysis. The ATP concentration was determined by high-performance liquid chromatography (HPLC, LC-1260, Agilent, USA), using a ZORBAX SB-C18 column (250 mm \times 4.6 mm \times 5 μm). The detector wavelength was set at 260 nm and 10 μL sample was injected. The mobile phase was a mixture of 20 mmol/L ammonium acetate (pH 4.5) and acetonitrile (5:95, v/v) at a flow rate of 1.0 mL/min.

5. AHLs assay

N-acylhomoserine lactones (AHLs) was measured according to the described protocol [4]. 20 mL samples were crushed by an ultrasonic cell crusher, and then centrifuged at 8000 rpm for 5 min. After filtration through 0.22 μm filter membranes, the supernatant was extracted with an equivalent volume of ethyl acetate. The extract was evaporated at 40 °C with a rotary evaporator (Yarong RE-5220, China), and then dissolved in methanol.

The AHLs concentration was detected using the Agilent 6410B UPLC-MS (Agilent, U.S.A.) with BEH C-18 column (50 mm \times 4.6 mm \times 1.8 μm). The mobile phase was a mixture of methanol and water. The nebulizer gas was N_2 and the flow rate of dryer gas was set at 9 L/min. The heated capillary and voltage were maintained at 350 °C and 4 kV, respectively.

Fig. S1. The acute toxicities of CLP toward the nitrate reduction in denitrification process.

Fig. S2. Tafel plot along a CLP gradient.

Fig. S3. (a) Effects of CLP concentration on the level of AHLs. Linear relationships between (b) C8-HSL, (c) C4-HSL, (d) C14-HSL and EPS in the recovery stage of denitrification. Error bars represent standard deviations of triplicate measurements.

Fig. S4. Average relative abundance of *Acinetobacter* and *Shinella* at different phases.

Fig.S1

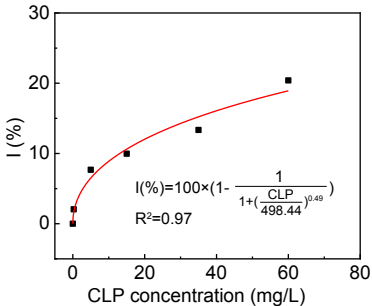


Fig.S2

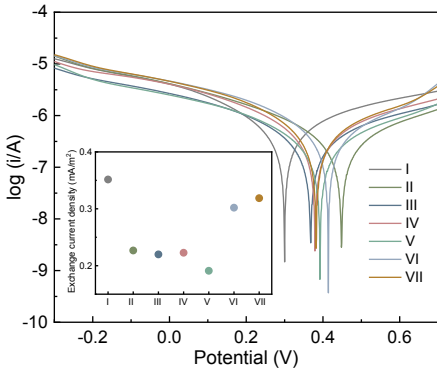


Fig.S3

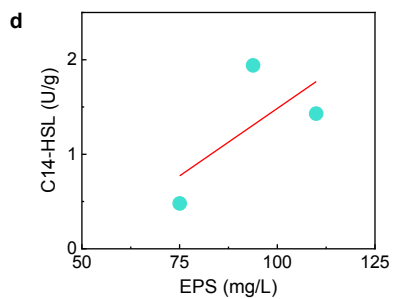
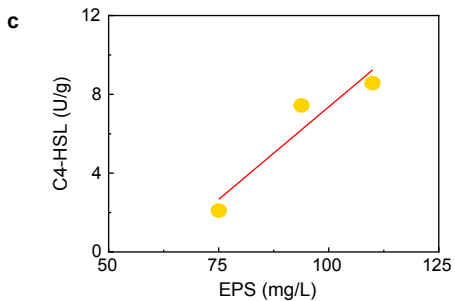
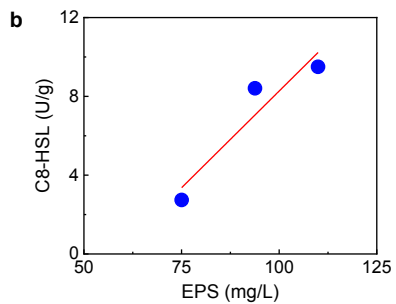
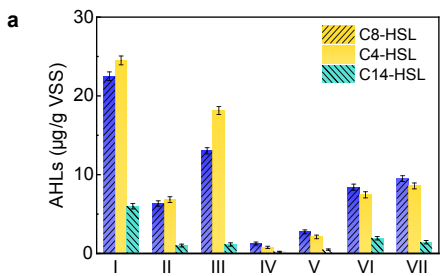


Fig.S4

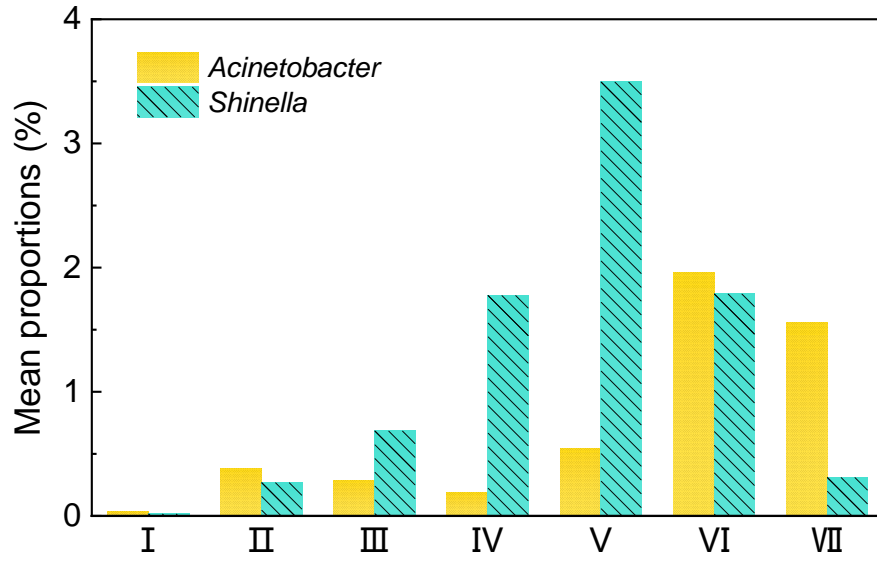


Table S1

Similarity-based OTUs and species richness and diversity estimate for denitrifying microbial communities from phase I to phase VII.

Phase	OTU	Coverage	Chao	Ace	Shannon
I	1487	0.99	1935.87	1926.77	5.37
II	1386	0.99	1941.81	1923.13	5.19
III	1352	0.99	1723.32	1746.75	5.10
IV	1322	0.99	1806.22	1874.26	5.01
V	1284	0.99	1637.00	1676.89	4.85
VI	1246	0.99	1697.08	1723.51	5.12
VII	1533	0.99	1769.15	1747.96	5.37

Table S2

Specific values of ROS, SOD, LDH, NAR, NIR, MDH, NADH, ATP, ETSA, EPS and AHLs.

Phase	ROS (U/g)	SOD (U/g)	LDH (U/g)	NAR (U/g)	NIR (U/g)	MDH (U/g)	NADH (U/g)	ATP (mg/g VSS)	ETSA (µg/(mg·h))	EPS (mg/g VSS)	C8-HSL (µg/g VSS)	C4-HSL (µg/g VSS)	C14-HSL (µg/g VSS)
I	4474.11 ±136.31	4372.71 ±182.57	39.60±2.2 0	1.46± 0.03	0.81± 0.04	2.45±0.12	1.89±0.07	2.57±0.07	2.80±0.06	92.28±5.21	22.51±0.55	24.55±0.56	6.12±0.34
II	4825.57 ±207.68	5964.26 ±282.54	43.97±2.3 9	1.56± 0.08	0.73± 0.04	2.22±0.14	1.70±0.11	1.53±0.07	2.20±0.03	110.05±4.9 1	6.33±0.35	6.83±0.37	1.01±0.18
III	5244.30 ±209.21	5603.27 ±328.54	49.08±3.2 0	1.47± 0.01	0.61± 0.04	2.05±0.12	1.53±0.11	0.99±0.06	2.00±0.02	85.90±4.85	13.03±0.39	18.13±0.51	1.13±0.21
IV	4863.52 ±200.16	5713.54 ±515.66	46.23±3.3 0	1.61± 0.06	0.65± 0.03	2.19±0.09	1.58±0.02	1.21±0.10	2.10±0.02	83.08±3.68	1.25±0.19	0.76±0.15	0.22±0.06
V	4752.15 ±101.65	5653.90 ±370.05	46.74±1.0 5	1.51± 0.04	0.56± 0.03	1.76±0.09	1.46±0.06	0.64±0.02	1.80±0.02	75.03±3.27	2.74±0.25	2.10±0.23	0.48±0.09
VI	4400.67 ±91.37	4674.03 ±287.34	41.74±1.7 9	1.48± 0.02	0.59± 0.03	2.17±0.12	1.50±0.06	1.34±0.06	2.22±0.03	93.81±4.82	8.41±0.39	7.44±0.39	1.94±0.23
VII	4456.54 ±111.69	4525.45 ±185.38	40.71±1.4 2192	1.66± 0.10	0.69± 0.04	2.20±0.11	1.74±0.08	1.44±0.05	2.50±0.05	109.97±5.7 0	9.51±0.37	8.57±0.38	1.43±0.22

References

- [1] J.T. Ji, Y.Z. Peng, B. Wang, W.K. Mai, X.Y. Li, Q. Zhang, S.Y. Wang, Effects of salinity build-up on the performance and microbial community of partial-denitrification granular sludge with high nitrite accumulation, *Chemosphere* 209 (2018) 53-60.
- [2] Y Xiao, E.H. Zhang, J.D. Zhang, Y.F. Dai, Z.H. Yang, H.E.M. Christensen, J. Ulstrup, F. Zhao, Extracellular polymeric substances are transient media for microbial extracellular electron transfer, *Sci. Adv.* 3(7) (2017) 1700623.
- [3] Y. He, J.B. Guo, Y.Y. Song, Z. Chen, C.C. Lu, Y. Han, H.B. Li, Y.N. Hou, R. Zhao, Acceleration mechanism of bioavailable Fe(III) on Te(IV) bioreduction of *Shewanella oneidensis* MR-1: promotion of electron generation, electron transfer and energy level, *J. Hazard. Mater.* 403 (2021) 123728.
- [4] T. Wang, J.B. Guo, Y.Y. Song, J. Lian, H.B. Li, C.C. Lu, Y. Han, Y.N. Hou, Efficient nitrogen removal in separate coupled-system of anammox and sulfur autotrophic denitrification with a nitrification side-branch under substrate fluctuation, *Sci. Total Environ.* 696 (2019) 133929.